How do the properties of amphiphilic polymer membranes influence the functional insertion of peptide pores?

Andrea Belluati[1] ‡, Viktoria Mikhalevich[1] ‡, Saziye Yorulmaz Avsar[1], Davy Daubian[1], Ioana Craciun[1], Mohamed Chami[2], Wolfgang Meier[1], Cornelia G. Palivan[1]**

[1]Department of Chemistry, University of Basel, Mattenstrasse 24a, BPR 1096, 4058 Basel, Switzerland

[2]BioEM lab, Biozentrum, University of Basel, Mattenstrasse 26, 4058 Basel, Switzerland

Supporting Information

S1. Planar membrane characterization and melittin interaction.

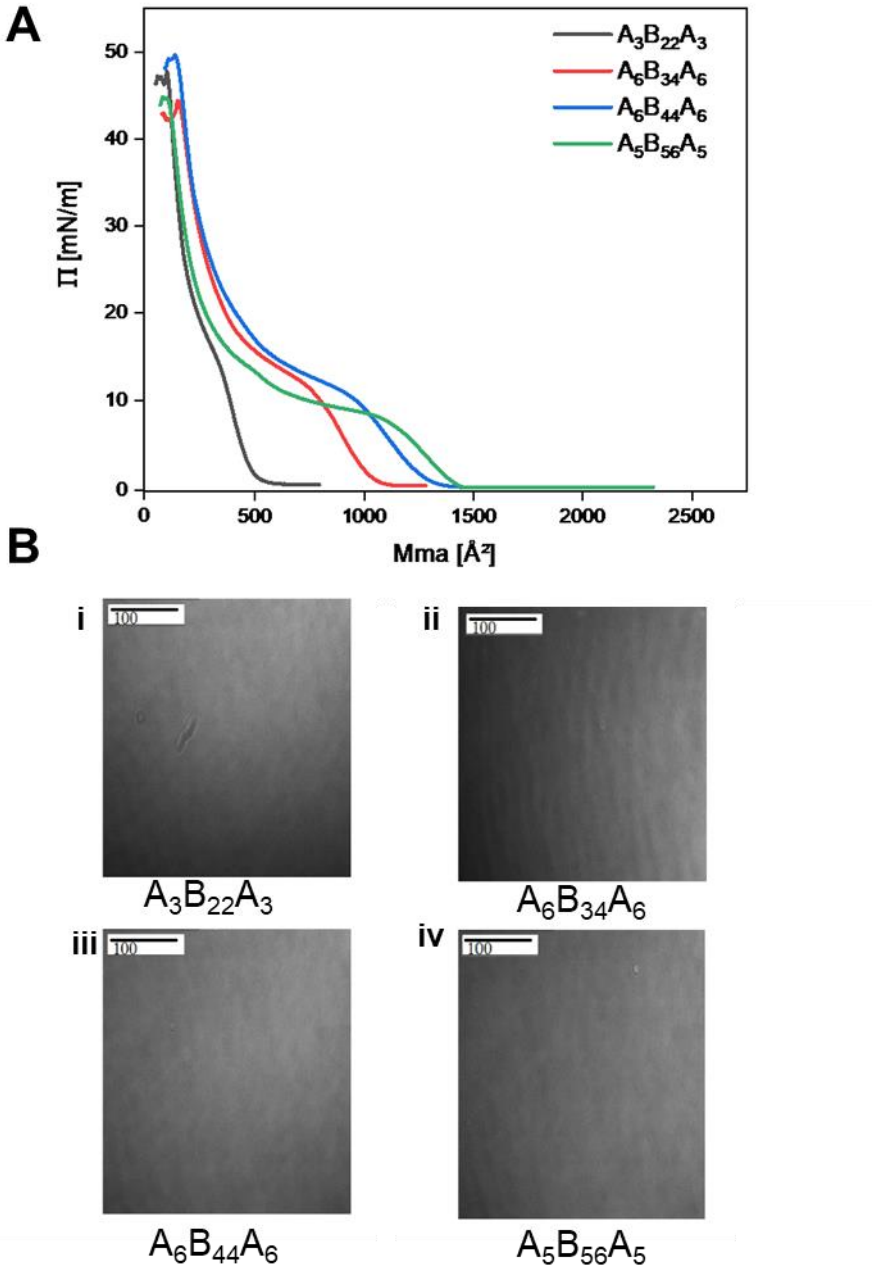

Figure S1. (A) Langmuir-Isotherms of the four polymers $A_6B_{44}A_6$, $A_6B_{34}A_6$,$A_3B_{22}A_3$ and $A_5B_{56}A_5$. B) BAM micrographs for the four polymers: i) $A_6B_{44}A_6$, ii) $A_6B_{34}A_6$,iii) $A_3B_{22}A_3$ and iv) $A_5B_{56}A_5$ at the surface pressures (38 mN m^{-1}) used for transfer. The scale bar (100 µm) is the same for all images.

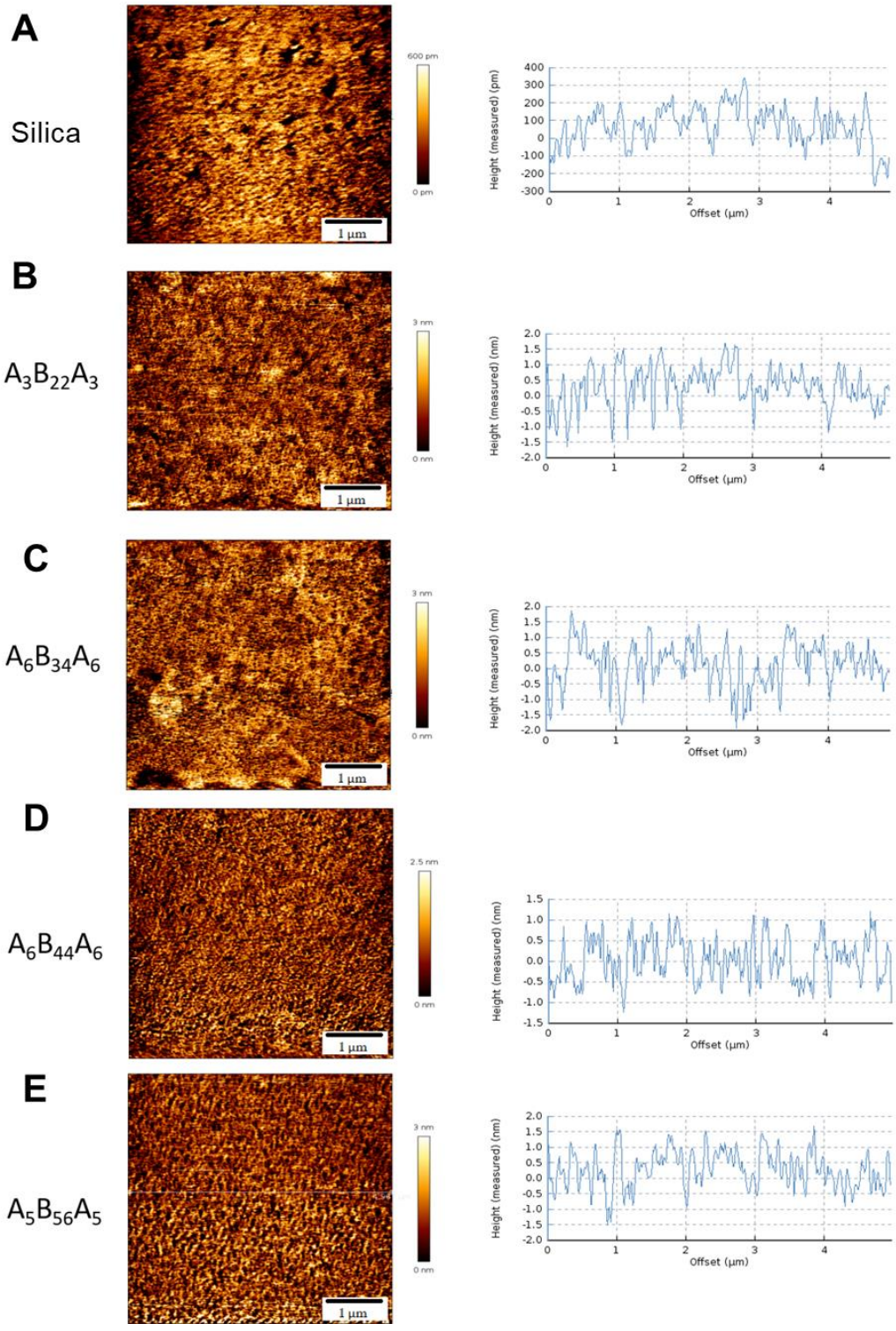

Figure S2. AFM micrographs and their respective cross sections for (A) silica and after deposition of (B) $A_3B_{22}A_3$, (C) $A_6B_{34}A_6$, (D) $A_6B_{44}A_6$ and (E)$A_5B_{56}A_5$ on silica.

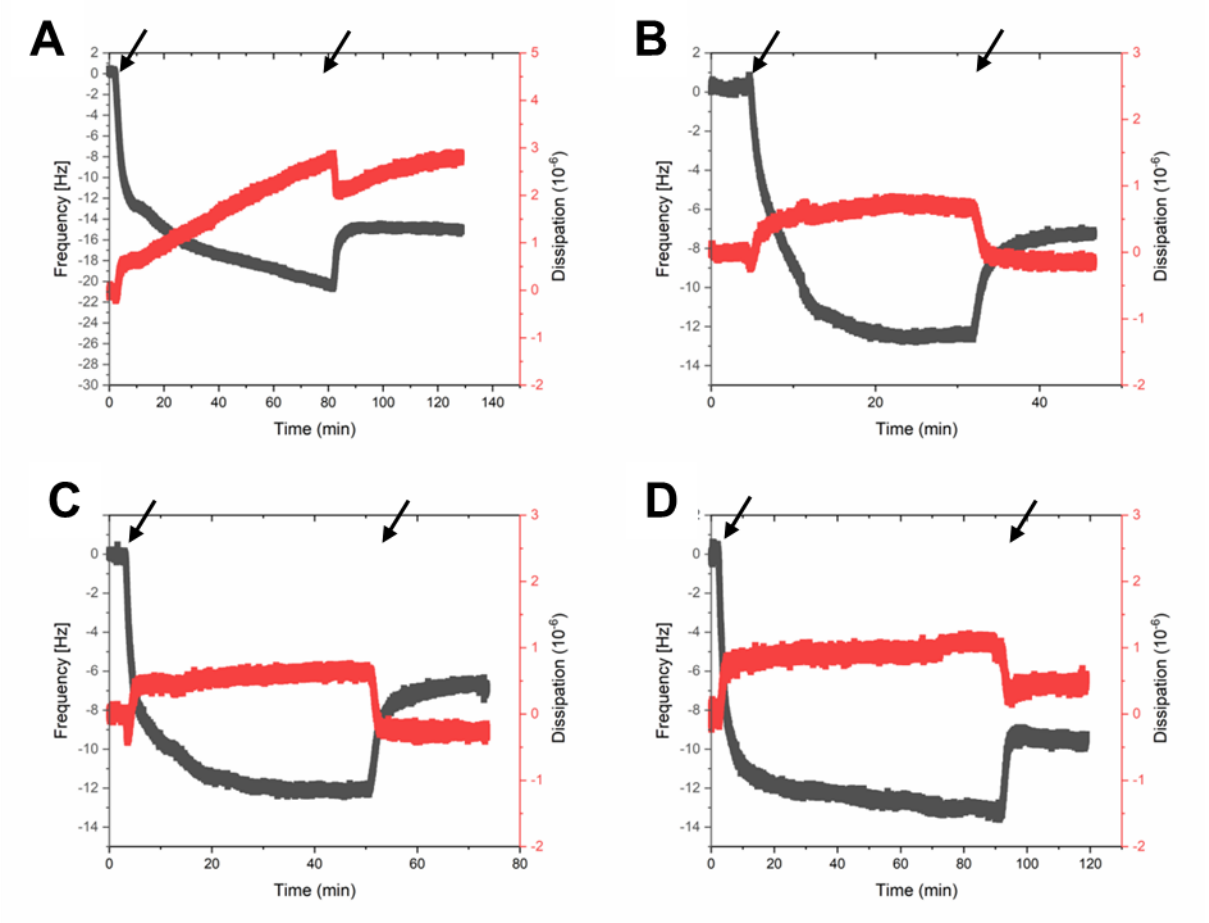

Figure S3. Changed in frequency and dissipation shift upon addition of 15 µM melittin to solid supported polymer membrane made of (A) $A_3B_{22}A_3$, (B) $A_6B_{34}A_6$, (C) $A_6B_{44}A_6$ and (D) $A_5B_{56}A_5$. The arrows sequentially indicate addition of melittin and rinsing with buffer solution.

S2. Functionality of melittin in planar membranes.

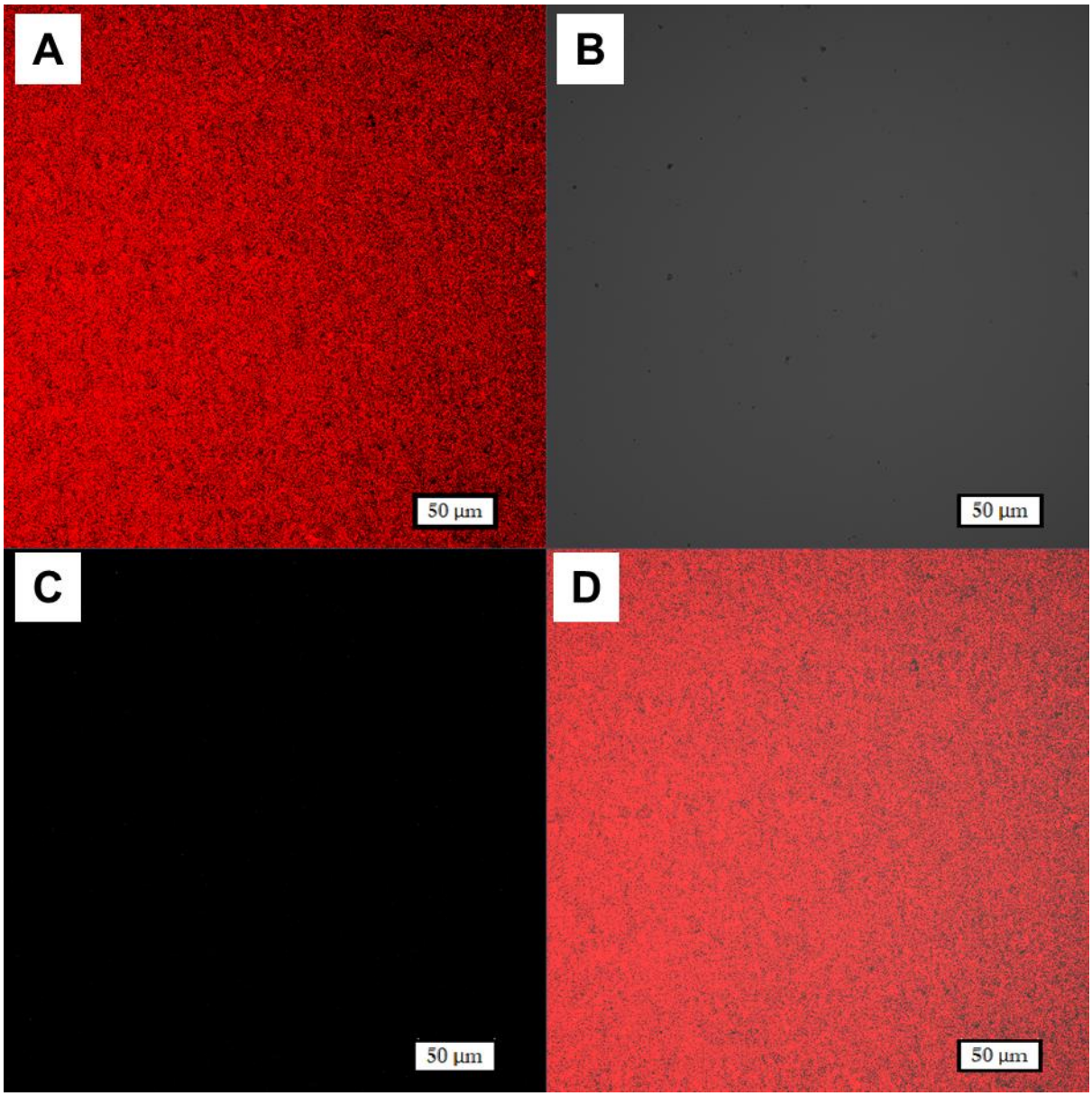

Figure S4. CLSM micrograph of a labelled $A_5B_{56}A_5$ membrane with the melittin/Alizarin Red with (A) labelled membrane (red), (B) transmission channel, (C) Alizarin channel (green) and (D) the combined channel for the labelled membrane and Alizarin. The scalebar is the same for all images (50 µm).

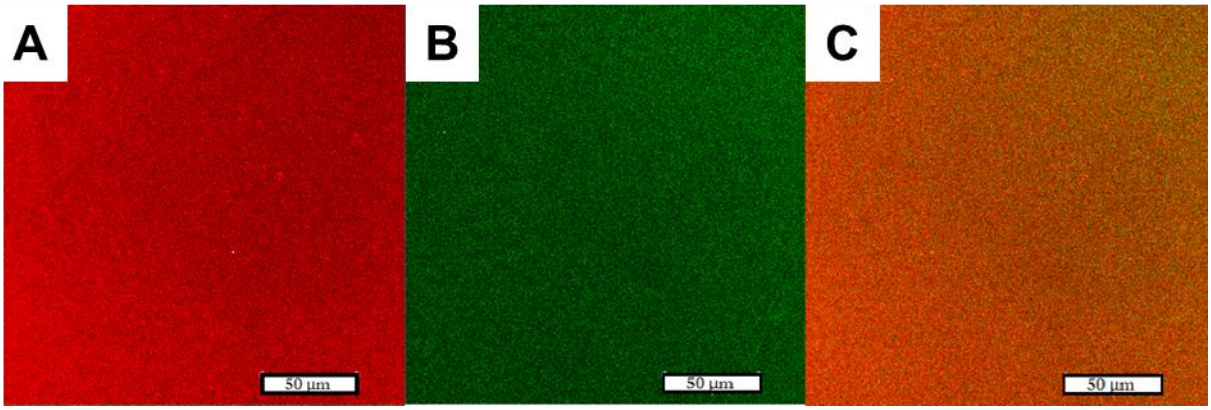

Figure S5. CLSM micrographs of a solid supported polymer membrane made of $A_3B_{22}A_3$ block copolymers with FITC labeled-melittin added before transfer (A) the SRB labeled-polymer channel (Red) , (B) the FITC labeled-melittin channel (green) and (C) the combination of both channels. The scale bar is the same for all images (50 µm).

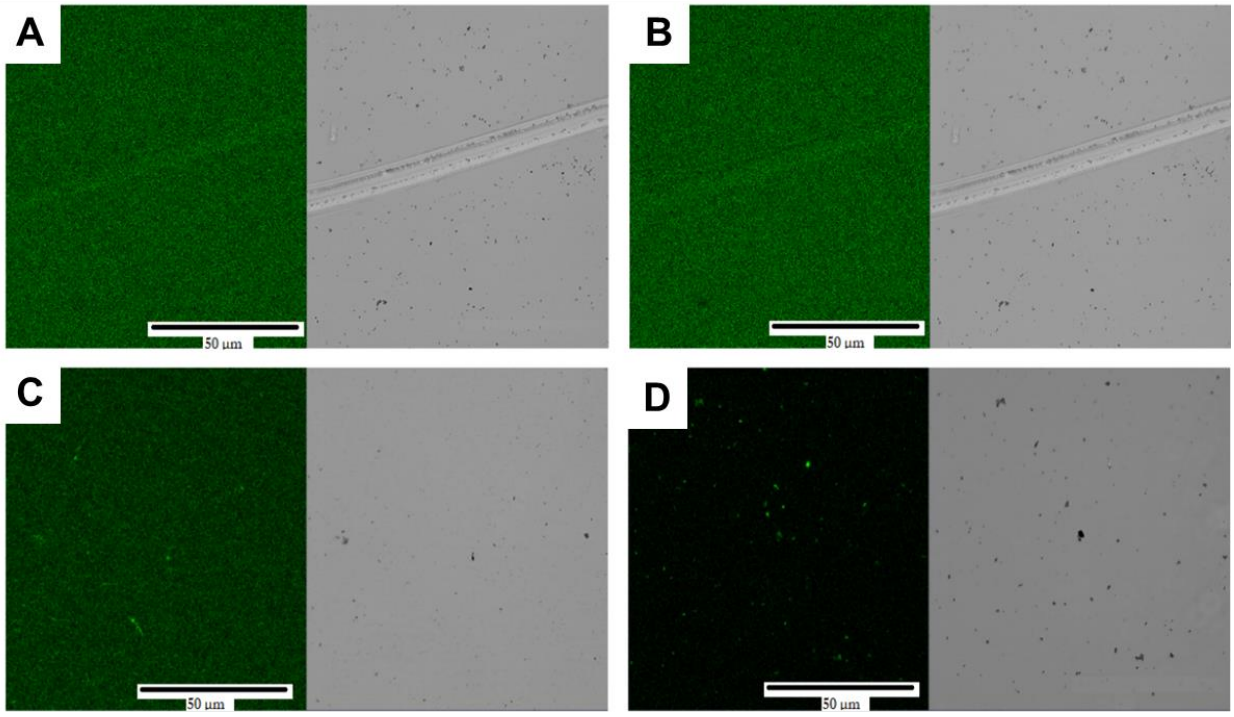

Figure S6. CLSM micrographs of polymer membranes made of $A_3B_{22}A_3$ on alizarin containing glass slides. (A) No melittin, before glucose addition, (B) no melittin, 1h after glucose addition, (C) melittin

was added before transfer, before glucose addition, (D) melittin was added before transfer, 1h after glucose addition. The scale bar is the same for all images (50 µm).

S3. Interaction of melittin with GUVs.

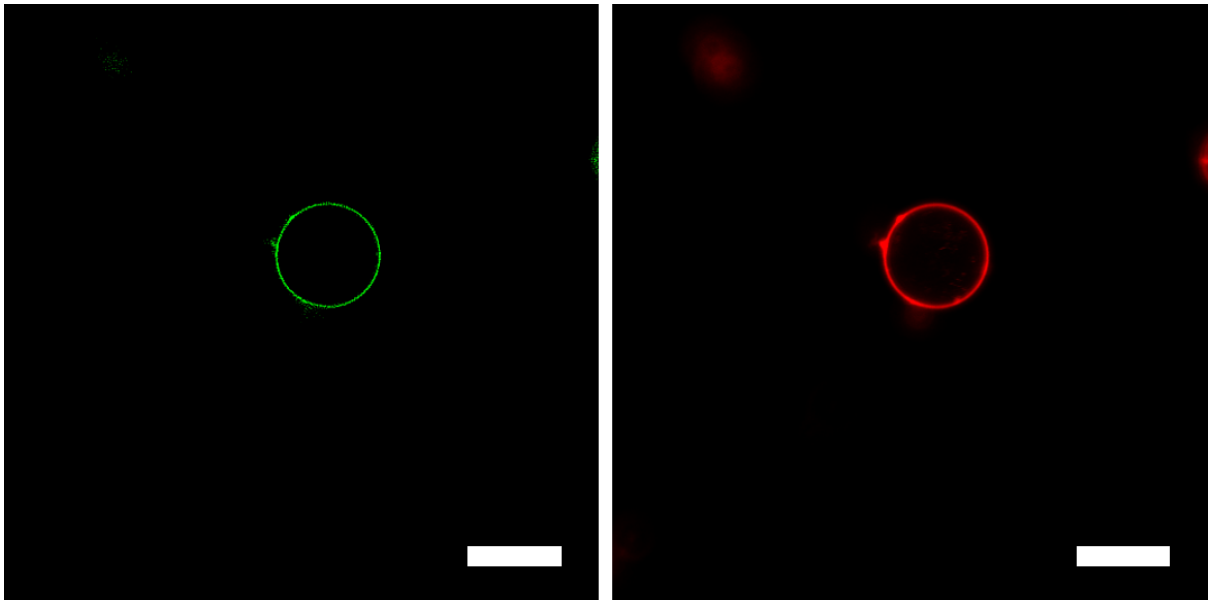

Figure S7. CLSM micrographs of GUVs FITC-melittin GUV. Green: FITC. Red: BODIPY 630/650. Scalebar: 5 µm.

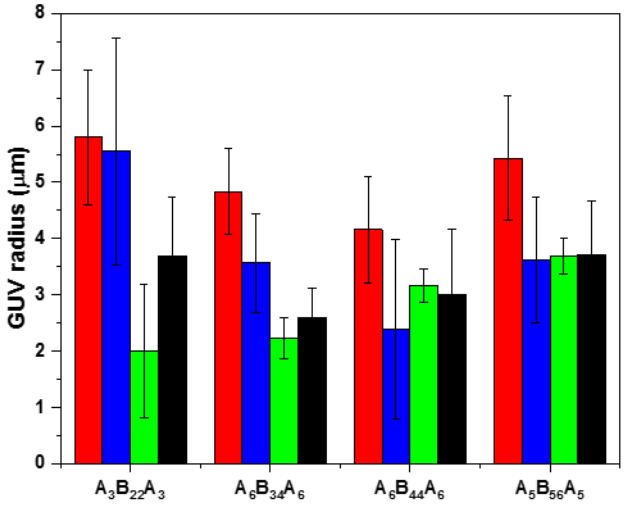

Figure S8. Radii of GUVs unpermeabilized, melittin in film (red), permeabilized, melittin in film (blue), unpermeabilized, melittin in buffer (green), permeabilized, melittin in buffer (black). As no appreciable difference can be observed, melittin does not change the radius of vesicles. Error bars given as ± SD, n = 3

S4. Polymersome characterization.

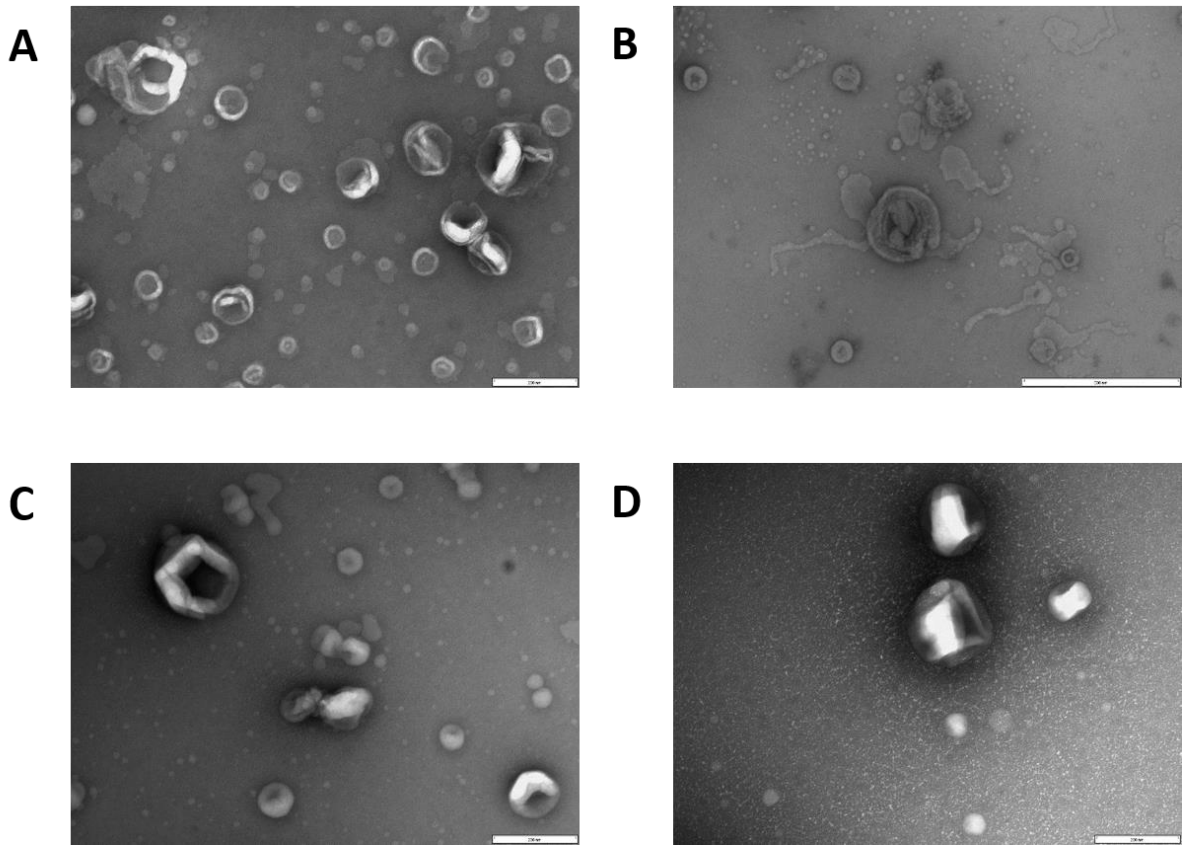

Figure S9. TEM micrographs of polymersomes. (A): $A_3B_{22}B_3$. (B): $A_6B_{34}B_6$. (C): $A_6B_{44}B_6$. (D): $A_5B_{56}B_5$. Scalebar: 200 nm.

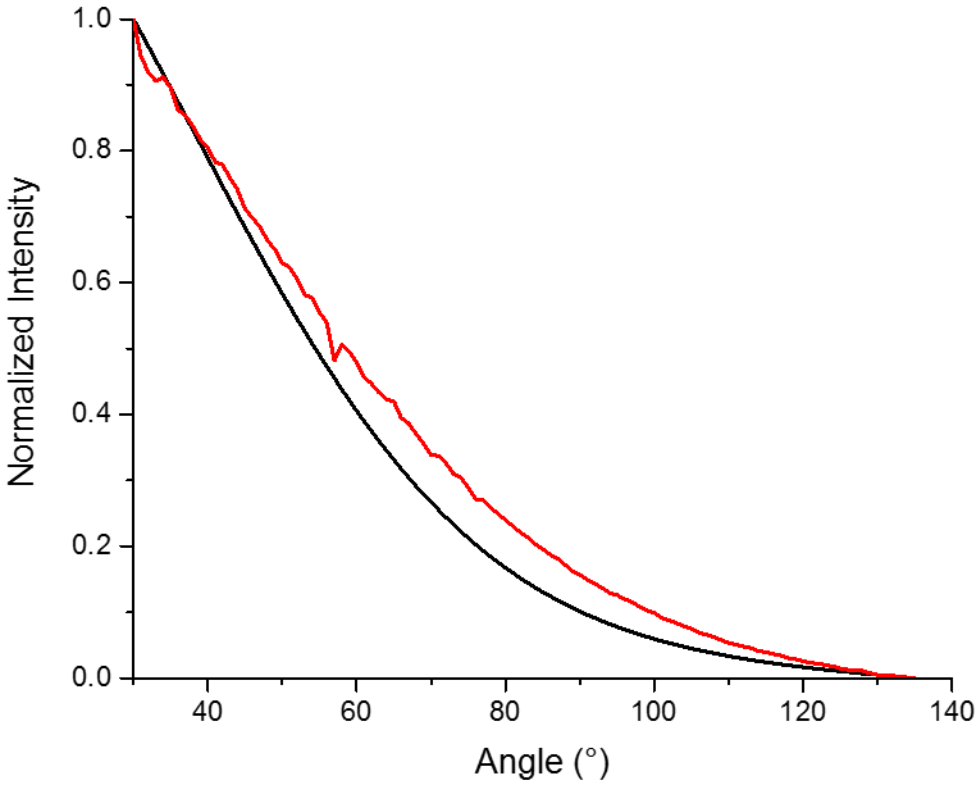

Figure S10. MIE plot (SLS) for $A_3B_{22}B_3$ (red) and simulated R=125 nm (black), angle dependency.

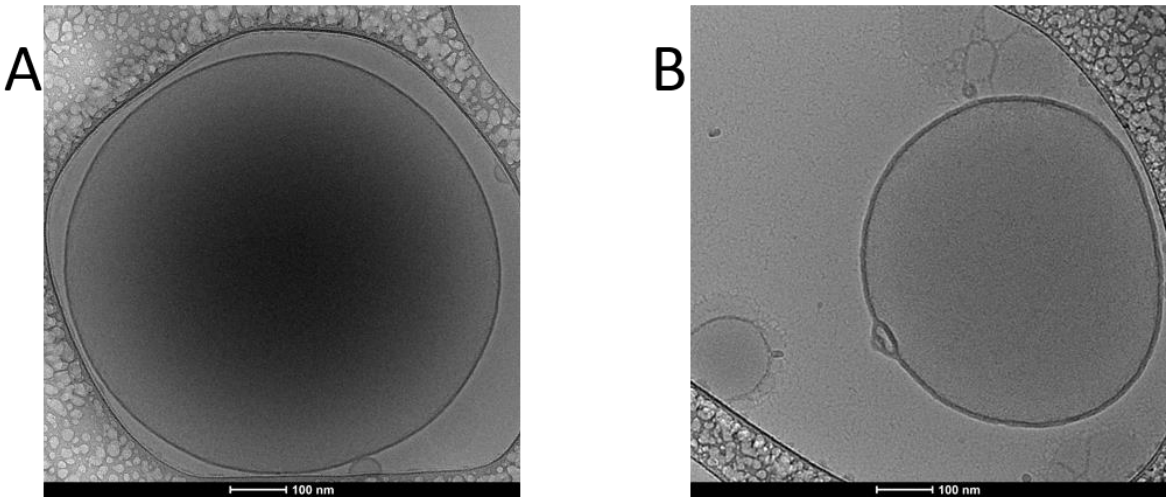

Figure S11. Cryo-TEM micrographs of GUVs and polymersomes. (A): $A_3B_{22}A_3$. (B): $A_5B_{56}A_5$.

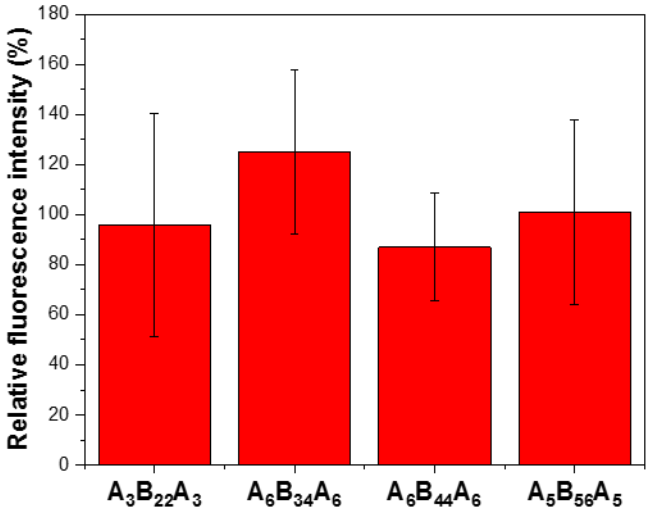

Figure S12. Relative fluorescence of SRB-filled polymersomes in PBS to polymersomes in sucrose. 100% intensity means no change in fluorescence.

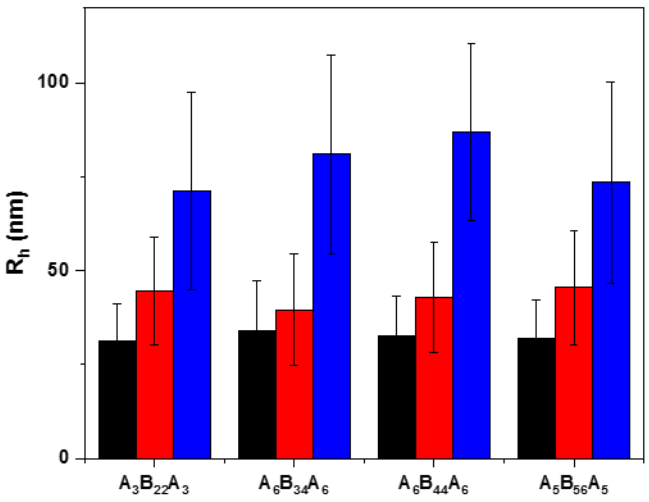

Figure S13. R_h of polymersomes, after extrusion at 50 nm (black), 100 nm (red), 200 nm (blue).

S5. Pore number estimation

Melittin pores are reported to be composed by 3 to 9 monomers[1]; if we assume assuming a tetrameric pore, with minimal size 1.3 nm, enough for SRB [2], we can estimate the maximal number of pores per vesicle, knowing the number of monomers per vesicle m_v

$$n_{max} = \frac{m_v}{4}$$

Which we can correct for the permeabilized fraction f, indicating how many of these monomers on a vesicle are actually in the correct conformation

$$n_{corr} = n \times f$$

Knowing the mean R_h allows us to build a linear regression curve to estimate the number of functional pores of a GUV, ranging from 71 ± 7 for melittin added in film to $A_3B_{22}A_3$ to 5 ± for melittin *ex post* 1.5 in $A_6B_{44}A_6$, which is in the same order of magnitude of what reported in the literature with melittin and related peptides [3-4]. (Figure S19 A) When melittin is added *ex post*, the number of pores decreases with the decrease of vesicle size (from 15 to 1 pore), since melittin has to spread among more vesicles (Figure S19 B).

Assuming that polymersomes behave similarly to GUVs with melittin and form pores in the same way, we see a discrepancy between theoretical pores/vesicle (melittin in film or in buffer) and permeabilization efficiency found in GUVs, smaller than what expected from such an amount of pores (Figure S19 C,D).

As previously mentioned, a possible explanation is that interaction with the membrane (measured by FCS) is only one factor in permeabilization, suggesting that there are other physico-chemical properties, namely membrane stiffness and thickness, playing a role; in phospholipids, the main differences arise from the different ratios of lipids.[5-7]

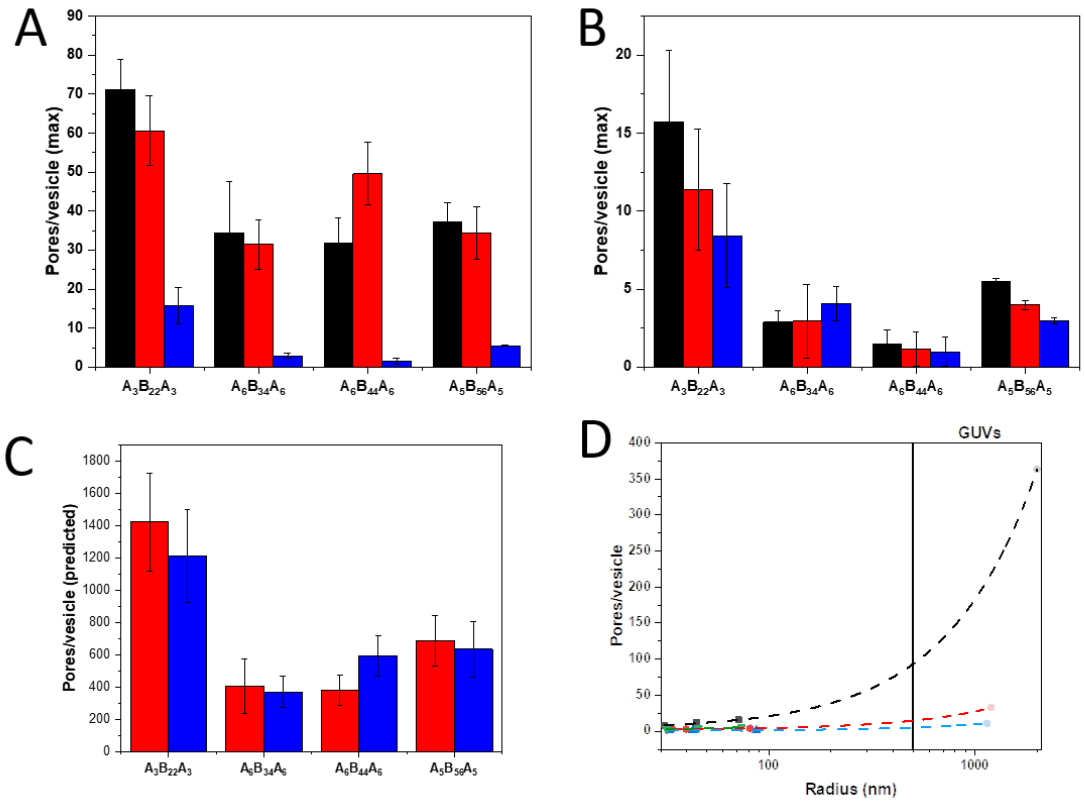

Figure S14. (A): maximal number of melittin pores per vesicles when melittin is added to the film (black), to the buffer (red), or ex post (blue). (B): maximal number of melittin pores per vesicles when melittin is added post at R_h 100 nm (black), 45 nm (red) and 30 nm (blue). (C): predicted number of pores per vesicle on GUVs with melittin added to the film (red) and to the buffer (blue). (D): regression curve of melittin per vesicle for polymersomes (left) and predicted number of pores for GUVs when melittin is added ex post (x axis in logarithmic scale). Error bars given as ± SD, n = 30.

REFERENCES

1. Fennouri, A.; Mayer, S. F.; Schroeder, T. B. H.; Mayer, M., Single channel planar lipid bilayer recordings of the melittin variant MelP5. *Biochimica et Biophysica Acta (BBA) - Biomembranes* **2017,** *1859* (10), 2051-2057.
2. Leveritt, J. M., 3rd; Pino-Angeles, A.; Lazaridis, T., The structure of a melittin-stabilized pore. *Biophys J* **2015,** *108* (10), 2424-2426.
3. Benachir, T.; Lafleur, M., Study of vesicle leakage induced by melittin. *Biochimica et Biophysica Acta (BBA) - Biomembranes* **1995,** *1235* (2), 452-460.
4. Arbuzova, A.; Schwarz, G., Pore-forming action of mastoparan peptides on liposomes: a quantitative analysis. *Biochimica et Biophysica Acta (BBA) - Biomembranes* **1999,** *1420* (1), 139-152.
5. Allende, D.; Simon, S. A.; McIntosh, T. J., Melittin-Induced Bilayer Leakage Depends on Lipid Material Properties: Evidence for Toroidal Pores. *Biophysical Journal* **2005,** *88* (3), 1828-1837.
6. Raghuraman, H.; Chattopadhyay, A., Orientation and dynamics of melittin in membranes of varying composition utilizing NBD fluorescence. *Biophysical journal* **2007,** *92* (4), 1271-1283.
7. van den Bogaart, G.; Guzman, J. V.; Mika, J. T.; Poolman, B., On the mechanism of pore formation by melittin. *J Biol Chem* **2008,** *283* (49), 33854-7.